Nd-ion Substitution Effect on f-electron Multipole Order of PrRu4P12

Physics Procedia

Volume 75, 2015, Pages 179–186

20th International Conference on Magnetism

Nd-ion substitution effect on f-electron multipole order of $PrRu_4P_{12}$

Kazuaki Iwasa[1], Ari Yonemoto[1], Shigeru Takagi[1], Shinichi Itoh[2], Tetsuya Yokoo[2], Soshi Ibuka[2], Chihiro Sekine[3], and Hitoshi Sugawara[4]

[1] Department of Physics, Tohoku University, Sendai, Miyagi 980-8578, Japan
[2] Neutron Science Division, Institute of Materials Structure Science, High Energy Accelerator Research Organization, Tsukuba, Ibaraki 305-0801, Japan
[3] Department of Electrical and Electronic Engineering, Muroran Institute of Technology, Muroran, Hokkaido 050-8585, Japan
[4] Department of Physics, Kobe University, Kobe, Hyogo 657-8501, Japan

Abstract

We studied the effect of magnetic Nd-ion substitution on the metal-nonmetal transition at a transition temperature of 63 K of $PrRu_4P_{12}$, which is characterized by antiferro-type electric multipole ordering of Pr-ion $4f$ electrons. The transition temperature of $Pr_{1-x}Nd_xRu_4P_{12}$ depends weakly on the Nd concentration x as compared to La- and Ce-substituted compounds. Inelastic neutron-scattering measurements revealed that the energies and widths of crystalline field excitation peaks of Pr $4f^2$ in $Pr_{0.85}Nd_{0.15}Ru_4P_{12}$ are very similar to those of $PrRu_4P_{12}$. These experimental results indicate that the ordered state is robust against the substitution of magnetic Nd ions as compared to the La and Ce substitutions. Magnetic interactions between the Pr ions and the Nd ions in $Pr_{1-x}Nd_xRu_4P_{12}$ help stabilize the magnetic triplet ground state of the Pr ions that appears in the antiferro-type multipole ordered phase. Therefore, the nonmagnetic multipole ordered phase of $PrRu_4P_{12}$ is compatible with the magnetic perturbation.

Keywords: Metal-nonmetal transition, Electron multipole, X-ray diffraction, Neutron scattering

1 Introduction

Electron multipoles have extended degrees of freedom relevant to strongly correlated electronic states. For the last two decades, high-rank multipoles of f electrons in rare-earth-filled skutterudite compounds have been found to be order parameters on the phase transition accompanying not only magnetic anomalies but also drastic variations in electrical conductivity, which originate from p–f hybridization between carriers provided by pnictogen atoms and rare-earth f electrons [1]. In particular, $4f^2$ electron configuration of Pr^{3+} ions under cubic point symmetry allows multipoles owing to degenerated crystalline-field (CF) levels without magnetic degrees of

Selection and peer-review under responsibility of the Scientific Programme Committee of ICM 2015

doi:10.1016/j.phpro.2015.12.193

freedom. $PrOs_4Sb_{12}$ is considered a heavy-fermion superconductor, which is neighbored by the magnetic field-induced quadrupole ordered phase [2, 3]. $PrFe_4P_{12}$ exhibits extreme electron-mass enhancement [4], which is caused by the Kondo effect associated with a singlet-triplet CF scheme [5, 6]. A nonmagnetic ordered phase transition at 6.5 K of this compound was recently interpreted as a staggered ordering of a localized Pr $4f$ site with a singlet ground state and a strongly hybridized site forming a Kondo singlet state [7, 8, 9].

$PrRu_4P_{12}$ undergoes a metal-nonmetal transition at a transition temperature $T_{\rm MI}$ of 63 K [10]. Such higher-temperature phase transitions are also attributed to p–f hybridization. The electronic state in the ordered phase has been microscopically identified by two experimental results. The crystal structure transforms from body-centered cubic (space group $Im\bar{3}$) above $T_{\rm MI}$ to simple cubic ($Pm\bar{3}$) below $T_{\rm MI}$, as evidenced in X-ray superstructure scattering at a wave vector $\boldsymbol{q} = (1, 0, 0)$ [11]. The nonmetallic phase has also been characterized by staggered alignment of two inequivalent $4f$ states at the Pr1 site with a CF singlet ground state and at the Pr2 site with a triplet ground state, whereas the ground state in the metallic disordered phase is uniformly a singlet state [12, 13].

The nonmetallic ordered phase is associated with a charge density wave assisted not only by the structural modulation but also by the staggered ordering of Pr $4f$ electrons [14, 15]. Based on the detailed structural analysis, the ordered phase is characterized by the breaking of translational symmetry while conserving the local Pr-ion site symmetry. This means that the electronic hybridization effect gives additional CF potential to the Pr $4f$ electrons, and the order parameter is a totally symmetric multipole with a rank of four or more.

There remains a question as to how the degenerated ground state at the Pr2 site responds to perturbation. In order to solve this problem, atomic substitution effects have been studied. Substitutions of Ce for Pr and of Rh for Ru induce reentrant-type metal-nonmetal transitions [17, 16]. The nonmetallic phase appears below approximately 40–50 K in systems with impurity concentrations of 10% or so, and it transforms to a metallic phase at temperatures below 10 K. This phenomenon is caused by a carrier-doping effect owing to the atomic substitution, which suppresses the Fermi-surface nesting condition. The nonmetallic phase becomes a metastable state appearing only in the intermediate temperature range [18]. Our next target is to investigate the magnetic-impurity effect, which can be examined by Nd-ion substitution.

2 Experimental procedure

Samples of $Pr_{1-x}R_xRu_4P_{12}$ were synthesized by the Sn-flux method [19]. The atomic compositions, x, are those of the initial materials prior to synthesis. For $NdRu_4P_{12}$, the magnetic susceptibility was measured by using commercial SQUID magnetometers, and the specific heat was measured by the thermal relaxation method in a temperature range above 1 K. A four-circle X-ray diffractometer installed at Tohoku University was used to determine the transition temperatures of $Pr_{1-x}Nd_xRu_4P_{12}$ from measurements of the superstructure reflections. The X-ray source of a Mo rotating anode was operated at 40 kV and 100 mA, and K_α radiation was selected by a pyrolytic graphite monochromator. Inelastic neutron-scattering (INS) measurements of $Pr_{1-x}R_xRu_4P_{12}$ (R = Ce, and Nd) were performed at the chopper neutron spectrometer HRC installed at the beam line BL12 of the Materials and Life Science Experimental Facility (MLF) of J-PARC. The incident neutron energy was 8.83, 30.6, and 94.5 meV. The full width at half maximum (FWHM) of the energy spectrum for the incident energy of 30.6 meV was 1.38 meV at the elastic scattering position. INS for $Pr_{1-x}La_xRu_4P_{12}$ were measured at the triple-axis neutron spectrometer TOPAN installed at the beam line 6G of the research reactor JRR-3 of Japan Atomic Energy Agency. The spectrometer was operated with the fixed energy of

scattered neutrons at 13.4 meV by using a pyrolytic graphite analyzer. A set of collimators was open-60′-60′-open, and the FWHM is 1.25 meV at the elastic scattering position. Sample temperatures were controlled by closed-cycle helium refrigerators.

3 Experimental results

3.1 X-ray diffraction and phase diagram

Figure 1 shows the temperature dependences of the X-ray superstructure diffraction intensities of the single-crystalline samples of $x = 0.05,\ 0.15$, and 0.20. We determined the transition temperatures to be 61.5, 58.0, and 57.1 K for $x = 0.05,\ 0.15$, and 0.20, respectively, from the emergence of the superstructure intensities.

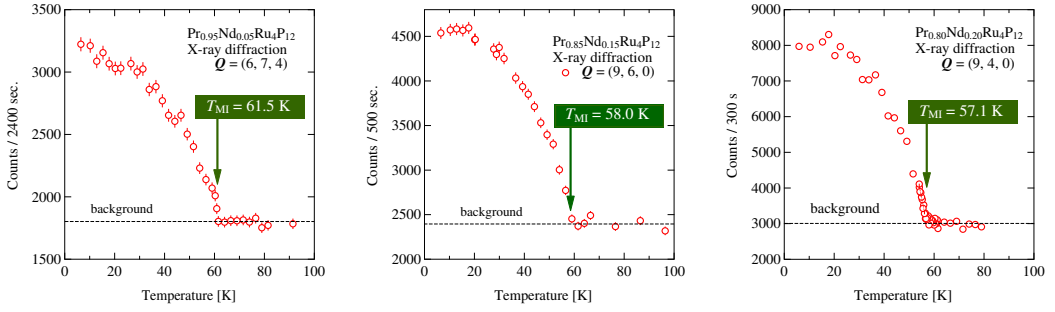

Figure 1: Temperature dependences of intensities of X-ray superstructure reflections of $Pr_{1-x}Nd_xRu_4P_{12}$ ($x = 0.05$, 0.15, and 0.20).

We summarize the metal-nonmetal transition temperatures of $Pr_{1-x}R_xRu_4P_{12}$ (R = La, Ce, and Nd) in Fig. 2. The transition temperatures of the La-substituted compounds, which were determined from the electrical resistivity data, are shown by open black diamonds [20]. The transition temperature decreases slightly with increasing La concentration. Because of the non-magnetic $4f^0$ configuration of La^{3+}, the decrease in transition temperature is attributed to a site-dilution effect, which disconnects the nearest-neighbor Pr-ion sites. The transition temperatures of the Ce-substituted compounds determined from the electrical resistivity data and the magnetic susceptibility data are shown as open squares [17], and those determined from the X-ray diffraction superstructure intensities are shown as solid squares [18]. There are two kinds of transition temperatures for the Ce-substituted compounds: T_{MI} above approximately 40 K and the reentrant transition point, T_R, below approximately 10 K. The decrease in T_{MI} for the Ce-substituted compounds is more rapid than that of the La-substituted compounds. As discussed previously, the Ce substitution induces a carrier-doping effect on the Fermi-surface nesting condition in $PrRu_4P_{12}$. This effect gives rise not only to the rapid suppression of T_{MI} as a function of the Ce concentration but also to the reentrant metallic phase appearing below T_R. The nonmetallic phase in the intermediate temperature range is no longer stable. Therefore, the Ce substitution forces the instability of the nonmetallic state as a consequence of the carrier-doping and the site-dilution effect.

The present experimental T_{MI} values of the Nd-substituted compounds are plotted as red solid circles. It is remarkable that the Nd-substituted compounds exhibit the highest transition temperature among these three rare-earth-substituted compounds, although the difference in

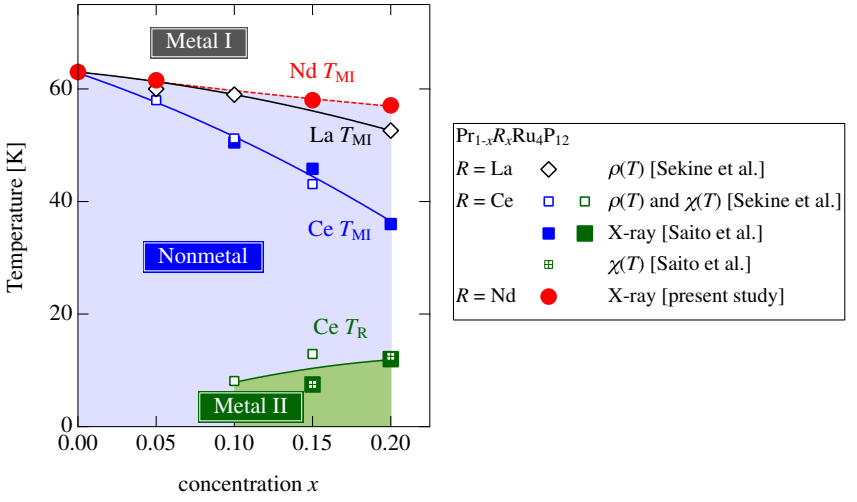

Figure 2: Phase diagram of $Pr_{1-x}R_xRu_4P_{12}$ (R = La, Ce, and Nd). The original data for the La- and Ce-substituted compounds are taken from Sekine et al. [17, 20] and Saito et al. [18].

T_{MI} between the La- and Nd-substituted compounds is subtle. The result indicates that the Nd substitution does not influence the ordering state as much as the Ce substitution because no modification to the carrier state is induced by the well-defined trivalent Nd ions.

3.2 Inelastic neutron scattering of $Pr_{1-x}R_xRu_4P_{12}$ (R = La, Ce, and Nd)

The antiferro-type ordered multipoles were identified by INS. As in a previous study on pure $PrRu_4P_{12}$, the temperature dependences of the peak energy and peak width of CF excitations of Pr-ion $4f$ electrons signify the emergence of the ordered multipoles [12]. In order to extract the $4f$ electron states in $Pr_{0.85}Nd_{0.15}Ru_4P_{12}$, we compared the spectra of this compound with those of $PrRu_4P_{12}$ obtained with the same neutron spectrometer setup. Figure 3 shows measured INS spectra. Figure 3(a) shows the data for $PrRu_4P_{12}$ measured at 7.3, 45, and 53 K, which are consistent with the previously results [12]. Figure 3(b) shows the results of $Pr_{0.85}Nd_{0.15}Ru_4P_{12}$ at 8.8, 44, and 56 K, together with the data for $Pr_{0.85}Ce_{0.15}Ru_4P_{12}$ at 10 K. The spectral shape and temperature evolution of $Pr_{0.85}Nd_{0.15}Ru_4P_{12}$ resemble those of $PrRu_4P_{12}$, whereas the spectrum of $Pr_{0.85}Ce_{0.15}Ru_4P_{12}$ at 10 K is somewhat closer to those of the pure and Nd-substituted systems at 44–45 K. CF excitation peaks of the Nd $4f^3$ state in $Pr_{0.85}Nd_{0.15}Ru_4P_{12}$ were not detected for all the sets of incident neutron energies because the Nd ions were less in number and carried smaller magnetic scattering cross sections than the Pr ions.

We also compare the INS data of $Pr_{0.85}La_{0.15}Ru_4P_{12}$ at 12, 48, and 63 K with those of $PrRu_4P_{12}$ at 13, 48, and 63 K, which were obtained by using the TOPAN spectrometer, as shown in Fig. 3(c) and (d). The peak energies at 12 and 48 K of $Pr_{0.85}La_{0.15}Ru_4P_{12}$ are smaller than those of $PrRu_4P_{12}$, whereas those at 63 K of both compounds are close to each other. In addition, the spectra of $Pr_{0.85}La_{0.15}Ru_4P_{12}$ are broader and have stronger tail intensities as compared to $PrRu_4P_{12}$. This discrepancy between the La-substituted and the pure compounds are in marked contrast to the resemblance between the Nd-substituted and the pure compounds.

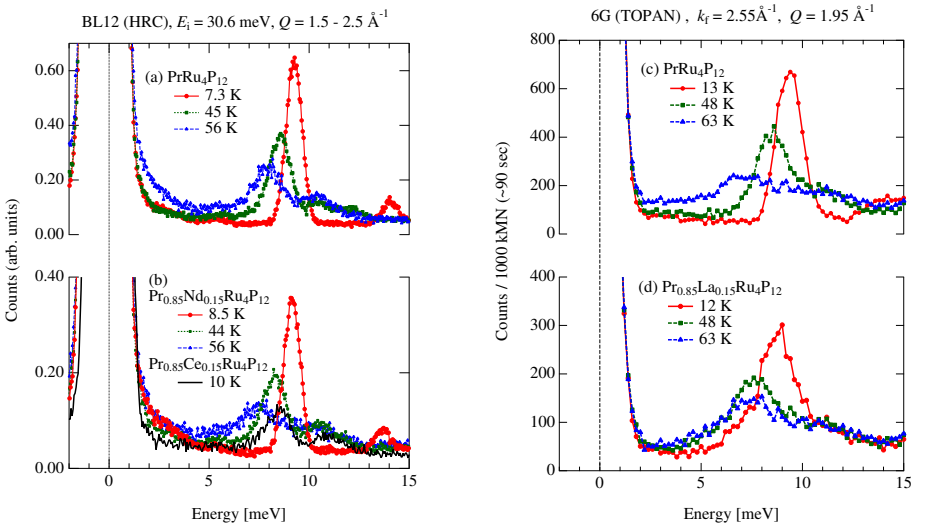

Figure 3: INS spectra of $PrRu_4P_{12}$ at 7.3, 45, and 53 K obtained by using the chopper spectrometer HRC (BL12 of MLF, J-PARC) are shown in (a). The data for $Pr_{0.85}Nd_{0.15}Ru_4P_{12}$ at 8.8, 44 and 56 K are shown in (b) together with $Pr_{0.85}Ce_{0.15}Ru_4P_{12}$ at 10 K. INS spectra of $PrRu_4P_{12}$ at 13, 48, and 63 K obtained by using the triple-axis spectrometer TOPAN (6G beam hole of JRR-3) are shown in (c). The data of $Pr_{0.85}La_{0.15}Ru_4P_{12}$ at 12, 48, and 63 K are shown in (d).

3.3 Specific heat and magnetic susceptibility of $NdRu_4P_{12}$

In order to discuss later the magnetic ground state of the Nd ions in $Pr_{0.85}Nd_{0.15}Ru_4P_{12}$, we have to identify the magnetic state of $NdRu_4P_{12}$. As described in a previous study, $NdRu_4P_{12}$ undergoes a ferromagnetic phase transition at low temperature [21]. Here, we show data of specific heat divided by temperature as a function of temperature in Fig. 4(a), which clearly shows a phase transition at 1.6 K. Assuming linear extrapolation of the specific heat down to 0 K, the magnetic entropy was evaluated to be $R \ln 4$ [J/(mol·K)] above the transition temperature, where R is the gas constant, as shown by a red solid line. Therefore, the CF ground state of a Nd ion is a quartet. The magnetic susceptibility of $NdRu_4P_{12}$ was measured under three sets of external magnetic fields applied along the [1 0 0] axis, as shown by the symbols in Fig. 4(b). The paramagnetic susceptibility data show a clear magnetic field dependence. These experimental data were analyzed on the basis of the mean-field model, as discussed later.

4 Analysis

In order to understand the Nd-substitution effect on the metal-nonmetal transition, we extracted the magnetic ground state of $NdRu_4P_{12}$ from the magnetic susceptibility data shown in Fig. 4. We adopt a simple mean-field model described by the following Hamiltonian equation.

$$\mathcal{H} = \mathcal{H}_{\rm CF} + K \langle \boldsymbol{J} \rangle \cdot \boldsymbol{J} - g_J \mu_{\rm B} \boldsymbol{J} \cdot \boldsymbol{H}, \tag{1}$$

where K is the exchange interaction energy for the magnetic moment $\boldsymbol{J}$ at the Nd-ion site. $\langle \boldsymbol{J} \rangle$ is the thermal-averaged magnetic moment, and thus we assume uniform nearest-neighbor

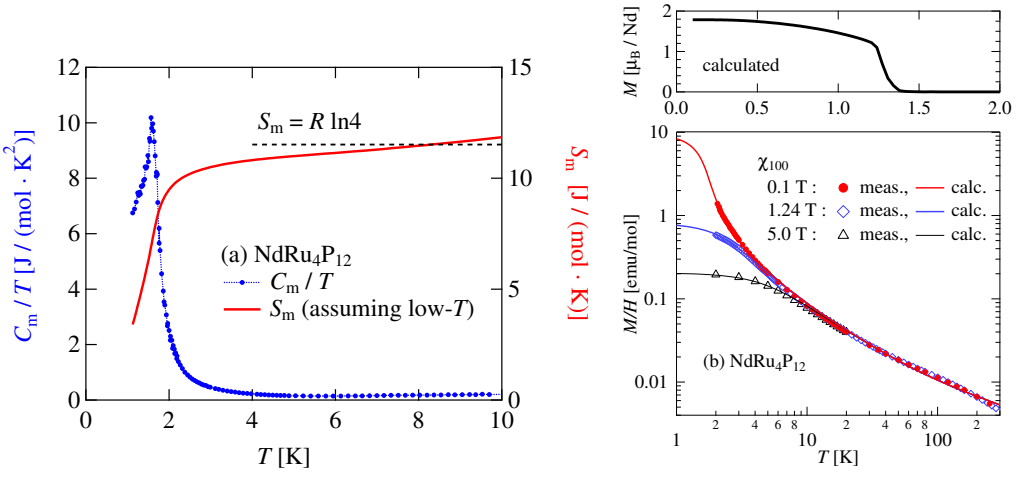

Figure 4: Magnetic specific heat divided by temperature (left ordinate) and magnetic entropy (right ordinate) are shown in (a). The symbols in (b) represent the magnetic susceptibility under magnetic fields of 0.1, 1.24, and 5.0 T applied parallel to the [100] axis of $NdRu_4P_{12}$. The lines are calculated results based on the mean-field approximation.

interaction, which covers the ferromagnetic state, as suggested previously. The last term in eq. 1 is a Zeeman term caused by the applied magnetic field $\boldsymbol{H}$. $\mathcal{H}_{\rm CF}$ represents a CF Hamiltonian for the $4f^3$ electron configuration of a Nd^{3+} ion under the point symmetry T_h of the rare-earth skutterudite structure [22].

$$\mathcal{H}_{\rm CF} = W\left[\frac{x}{F_4}(O_4^0 + 5O_4^4) + \frac{1-|x|}{F_6^c}(O_6^0 - 21O_6^4) + \frac{y}{F_6^t}(O_6^2 - O_6^6)\right], \qquad (2)$$

where O_m^n expresses a Stevens' operator equivalent. The last term with y is caused by the lack of point symmetry C_4 in T_h for the filled skutterudite compounds. We take $F_4 = 60, F_6^c = 2520$, and $F_6^t = 240$ for the $Nd^{3+}4f^3$ state, as defined in the reference.

A least-squares fitting analysis based on solving the Hamiltonian to the magnetic susceptibility data was carried out. The results are shown by the lines in the right panel of Fig. 4(b), and they are well in accordance with the experimental data. The obtained parameters are $K = -0.0708$ meV for the ferromagnetic exchange interaction and $W = -1.71$ meV, $x = -0.360$, and $y = 0.149$ for the CF Hamiltonian. This parameter set gives a spontaneous ferromagnetic ordered component of $1.8\mu_B$/Nd appearing below 1.3 K, as shown in the left upper panel of Fig. 4(b), which is consistent with the previous investigation of the ferromagnetic transition temperature at 1.6 K [21]. The magnetic ground state of the CF level of the $Nd^{3+}4f^3$ state is the $\Gamma_{67}^{(2)}$ quartet state, which is also consistent with the magnetic entropy data. Excited CF levels are located above 60 meV, which do not contribute to the low-temperature properties.

5 Discussion

The CF excitation spectra of $Pr_{0.85}La_{0.15}Ru_4P_{12}$ deviate significantly from those of the pure system $PrRu_4P_{12}$, as shown in Fig. 3(c) and (d). In the case of $PrRu_4P_{12}$, the excitation from

the Γ_1 ground state to the excited state $\Gamma_4^{(1)}$ at the Pr1 site are observed as the peaks at 9.4, 8.4, and 7.2 meV at 13, 48, and 63 K, respectively. On the other hand, the same excitations of $Pr_{0.85}La_{0.15}Ru_4P_{12}$ are the peaks at 8.6, 7.6, and 7.4 meV at 12, 48, and 63 K, respectively. The peak shifts from 63 K in $Pr_{0.85}La_{0.15}Ru_4P_{12}$ are smaller than those in $PrRu_4P_{12}$. The peak-shift magnitude indicates the evolution of the multipole order parameter, which corresponds to potential energy of the Pr $4f$ electrons owing to p–f hybridization. The smaller shift of the INS peaks in $Pr_{0.85}La_{0.15}Ru_4P_{12}$ indicates suppression of the order parameter. Moreover, the spectra of $Pr_{0.85}La_{0.15}Ru_4P_{12}$ are broader than those of $PrRu_4P_{12}$. Mobile carriers make the CF peak broader, as seen in the data for the high-temperature metallic phase. Therefore, the broader spectra of $Pr_{0.85}La_{0.15}Ru_4P_{12}$ indicates that carriers remain even at low temperature in the ordered phase, which is consistent with the suppression of the order parameter accompanied by imperfect gap formation.

Contrary to the La substitution, the INS spectra of $Pr_{0.85}Nd_{0.15}Ru_4P_{12}$ are almost identical to those of $PrRu_4P_{12}$ across the whole measurement temperature range, as shown in Fig. 3(a) and (b). Considering the discussion for $Pr_{0.85}La_{0.15}Ru_4P_{12}$ given above, $Pr_{0.85}Nd_{0.15}Ru_4P_{12}$ carries almost the same magnitudes of order parameter and low carrier concentration as $PrRu_4P_{12}$. It is in marked contrast to the carrier-doping effect on the spectral shape of $Pr_{0.85}Ce_{0.15}Ru_4P_{12}$ at 10 K shown in the same figure. These INS data support the unexpected robustness of the nonmetallic phase against the Nd substitution. This robustness is consistent with the Nd-ion concentration dependence of T_{MI}, which is smaller than the concentration dependence of the La- and Ce-substituted compounds, although the difference between the Nd and the La substitution is not significant.

As mentioned above for the analysis of $NdRu_4P_{12}$, the CF ground state of the Nd $4f^3$ configuration is a quartet $\Gamma_{67}^{(2)}$, and the excited states are considered to be located above 60 meV. Because of the high-energy excited levels, we can hypothesize a similar electronic state even for the Nd ions substituted in $PrRu_4P_{12}$. Therefore, it is naturally expected that the magnetic moment originating from $\Gamma_{67}^{(2)}$ interacts with the magnetic moment of the triplet state at the Pr2 site, which becomes the ground state below approximately 40 K with the evolution of the order parameter. The Pr2–Nd interaction can assist in the stabilization of the Pr2-site triplet state, and the site-dilution effect might be cancelled out. The quartet $\Gamma_{67}^{(2)}$ state of the Nd ions carries not only a magnetic moment but also multipoles. These multipoles may also interact with the Pr2 $4f$ electron state and contribute to stabilizing the ordering. It is a future subject to extract such Pr2–Nd multi-interaction effects on the ordered phase of $PrRu_4P_{12}$.

6 Summary

The effect of magnetic Nd-ion substitution on the metal-nonmetal transition at $T_{MI} = 63$ K of $PrRu_4P_{12}$ was investigated. The antiferro-type electric multipole ordering of Pr-ion $4f$ electrons was less suppressed by the Nd substitution as compared to the nonmagnetic La substitution inducing the site-dilution effect. Based on the analysis of the ground state of $NdRu_4P_{12}$, the Nd ions in $Pr_{1-x}Nd_xRu_4P_{12}$ possess a magnetic moment that can interact with the Pr ions with a magnetic triplet ground state. Such inter-rare-earth interaction forces the development of a robust ordered state against atomic substitution. Because the high-rank multipole with highly degenerated levels appears under the cubic point symmetry, various channels of interaction of Pr ions can assist the nonmetallic ordered phase.

Acknowledgments

L. Hao, K. Saito, T. Sato, T. Hasegawa, N. Kimura, and N. Kabeya are acknowledged for their contributions to the study of $Pr_{1-x}R_xRu_4P_{12}$ (R = La and Ce). K. Tomiyasu and M. Onodera are acknowledged for their support during this study. The experiments performed at JRR-3 were conducted by the Joint-use Research Program for Neutron Scattering, ISSP, The University of Tokyo. The experiments performed at J-PARC were approved by the Neutron Scattering Program at the MLF Pulsed Neutron and Muon Source at J-PARC (2012A0014, 2012B0115, and 2014A0208). This study was supported in part by the Ministry of Education, Culture, Sports, Science and Technology (MEXT) of Japan through KAKENHI (20102005) and by Japan Society for the Promotion of Science (JSPS) through by KAKENHI (21224008, 23244068, and 24654080).

References

[1] Sato H, Sugawara H, Aoki Y, Harima H. Magnetic Properties of Filled Skutterudites. In: Buschow KHJ ed. *Handbook of Magnetic Materials Vol 18*, Amsterdam: North-Holland; 2009, p. 1.

[2] Bauer ED, Frederick NA, Ho P-C, Zapf VS, Maple MB. *Phys Rev B* 2002;**65**:100506.

[3] Kohgi M, Iwasa K, Nakajima M, Metoki N, Araki S, Bernhoeft N, Mignot J-M, Gukasov A, Sato H, Aoki Y, Sugawara H. *J Phys Soc Jpn* 2003;**72**:1002.

[4] Sugawara H, Matsuda TD, Abe K, Aoki Y, Sato H, Nojiri S, Inada Y, Settai R, Ōnuki Y. *Phys Rev B* 2002;**66**:134411.

[5] Otsuki J, Kusunose H, Kuramoto Y. *J Phys Soc Jpn* 2005;**74**:200.

[6] Otsuki J, Kusunose H, Kuramoto Y. *J Phys Soc Jpn* 2005;**74**:2082.

[7] Hoshino S, Otsuki J, Kuramoto Y. *J Phys Soc Jpn* 2010;**79**:074720.

[8] Hoshino S, Otsuki J, Kuramoto Y. *J Phys Soc Jpn* 2011;**80**:033703.

[9] Iwasa K, Hao L, Kohgi M, Kuwahara K, Mignot J-M, Sugawara H, Aoki Y, Matsuda TD, Sato H. *J Phys Soc Jpn* 2012;**81**:094711.

[10] Sekine C, Uchiumi T, Shirotani I, Yagi T. *Phys Rev Lett* 1997;**79**:3218.

[11] Lee CH, Matsuhata H, Yamaguchi H, Sekine C, Kihou K, Suzuki T, Noro T, Shirotani I. *Phys Rev B* 2004;**70**:153105.

[12] Iwasa K, Hao L, Kuwahara K, Kohgi M, Saha SR, Sugawara H, Aoki Y, Sato H, Tayama T, Sakakibara T. *Phys Rev B* 2005:**72**;024414.

[13] Iwasa K, Hao L, Hasegawa T, Takagi T, Horiuchi K, Mori Y, Murakami Y, Kuwahara K, Kohgi M, Sugawara H, Saha SR, Aoki Y, Sato H. *J Phys Soc Jpn* 2005:**74**;1930.

[14] Kuramoto Y, Otsuki J, Kiss A, Kusunose H. *Proc Theo Phys Suppl* 2005;**160**:134.

[15] Takimoto T. *J Phys Soc Jpn* 2006;**75**:034714.

[16] Sekine C, Hoshi N, Shirotani I, Matsuhira K, Wakeshima M, Hinatsu Y. *Physica B* 2006;**378-380**:211.

[17] Sekine C, Takusari M, Yagi T. *J Phys Soc Jpn* 2011;**80**:SA024.

[18] Saito K, Laulhé C, Sato T, Hao L, Mignot J-M, Iwasa K. *Phys Rev B* 2104;**89**:075131.

[19] Torikachvili MS, Chen JW, Dalichaouch Y, Guertin RP, McElfresh MW, Rossel C, Maple MB, Meisner GP. *Phys Rev B* 1987;**36**:8660.

[20] Sekine C, Inaba T, Kihou K, Shirotani I. *Physica B* 2000;**281**&**282**:300.

[21] Masaki S, Mito T, Wada S, Sugawara H, Kikuchi D, Sato H. *Phys Rev B* 2008;**78**:094414.

[22] Takegahara K, Harima H, Yanase A. *J Phys Soc Jpn* 2001;**70**:1190. 2001;**70**:3468. 2002;**71**:372.